Colloids and Surfaces B: Biointerfaces 114 (2014) 201–208

Contents lists available at ScienceDirect

Colloids and Surfaces B: Biointerfaces

journal homepage: www.elsevier.com/locate/colsurfb

Characterization and bacterial adhesion of chitosan-perfluorinated acid films

Karina L. Bierbrauer[a,b], Roxana V. Alasino[a,b], Adrián Muñoz[a], Dante M. Beltramo[a,b], Miriam C. Strumia[c,*]

[a] Centro de Excelencia en Productos y Procesos de Córdoba, Gobierno de la Provincia de Córdoba, Pabellón CEPROCOR, CP 5164, Santa María de Punilla, Córdoba, Argentina
[b] Consejo Nacional de Investigaciones Científicas y Técnicas, CONICET, Argentina
[c] Departamento de Química Orgánica, IMBIV, Facultad de Ciencias Químicas, Universidad Nacional de Córdoba, Ciudad Universitaria, CP 5000, Córdoba, Argentina

ARTICLE INFO

Article history:
Received 9 April 2013
Received in revised form 2 September 2013
Accepted 9 October 2013
Available online xxx

Keywords:
Chitosan
Perfluorinated acids
Thermal degradation
Rheology
Microbiological activity

ABSTRACT

We reported herein the study and characterization of films obtained by casting of chitosan solutions in perfluorinated acids, trifluoroacetic (TFA), perfluoropropionic (PFPA), and perfluorooctanoic (PFOA). The films were characterized by FTIR, solid state ^{13}C NMR, X-ray, AFM, contact angle, thermogravimetric effluent analysis by mass spectrometry, and rheology. The results showed a marked influence of chain length of the perfluorinated acids on the hydrophobic/hydrophilic ratio of the modified chitosan films which was evidenced by the different characteristics observed.

The material that showed greater surface stability was chitosan-PFOA. Chitosan film with the addition of PFOA modifier became more hydrophobic, thus water vapor permeability diminished compared to chitosan films alone, this new material also depicted bacterial adhesion which, together with the features already described, proves its potential in applications for bioreactor coating.

1. Introduction

Natural polymers are increasingly used in many technological applications for being renewable and ecological resources. Chitosan, the deacetylated version of chitin and the most abundant naturally occurring amino-polysaccharide, has attracted attention because of its unique physicochemical characteristics and biological activities [1].

In addition to the inherent properties of chitosan itself, many studies have been carried out aimed at expanding its range of application. In this regard, various ways of modification have been proposed, taking advantage of the reactivity of amino groups to form covalent bonds or electrostatic interactions with different reactive compounds used as modifiers [2,3]. The nature of the modification will determine the properties of the resulting material. For example, chitosan can be modified by the addition of hydrophobic compounds that react with the hydrophilic groups of the biopolymer. This is the case of fluorinated compounds that, as demonstrated, give new properties to the polymer reactivity, solubility and adhesion [2–7].

As previously described [8,9], trifluoroacetic acid proves a suitable solvent for the solubilization of chitosan and cellulose. Such solubilization allows the collection of blends where chitosan enhances the mechanical properties of cellulose. The dissolution of chitosan is also used as an additive in hair cosmetics, where the addition of trifluoroacetic acid prevents particle agglutination once the product is sprayed [10]. These studies are based on the formation of highly soluble salts between chitosan and trifluoroacetic acid via the amino groups of the former. Moreover, electrospun technique [5] applied to chitosan in TFA generated highly uniform nano-fibers, whose nano-structure persisted after neutralization. All these studies constitute a major contribution in the area of biopolymers modified with fluorinated substituents, especially nano-particles, fibers and, to a lesser extent, films.

In the present work, we are interested in the study and characterization of the properties of films obtained by casting solutions of chitosan in perfluorinated acids of different chain lengths, such as trifluoroacetic acid (TFA), perfluoropropionic acid (PFPA) and perfluorooctanoic acid (PFOA). In order to determine the new properties of the resulting materials, the evaluation was made directly on the films obtained. The results allowed determining the type of interactions (hydrophilic or hydrophobic) prevailing in the material after the incorporation of perfluorinated substituent in the polymeric structure; in addition, the properties of the microbiological

* Corresponding author. Tel.: +54 351 4334170/73x120; fax: +54 351 4333030.
E-mail address: mcs@fcq.unc.edu.ar (M.C. Strumia).

0927-7765/$ – see front matter © 2013 Elsevier B.V. All rights reserved.
http://dx.doi.org/10.1016/j.colsurfb.2013.10.013

activity arising from this modification could also be assessed. In this sense, we analyzed the viability of *Pseudomonas aeruginosa*, an opportunistic pathogen, against chitosan modified by pentadecafluorooctanoic acid (PFOA). This bacterium has been widely used to correlate the material surface properties with bacterial adhesion, as it can infect a broad range of hosts from amoeba to humans and associated with severe burns, cystic fibrosis, AIDS and cancer [11–14]. Once bacteria attach to a substratum surface, a multistep process leads to the formation of a complex and heterogeneous biofilm [12 and references therein]. On the one hand, biofilms can be detrimental for many devices; however, they can be beneficial to the degradation of environmental hazardous substances in a bioreactor. In the latter case, we should consider enhancing the initial attachment of bacteria to a substratum and keeping biofilms in a suitable spatial arrangement of different microbial species so as to stimulate an efficient degradation of specific substances in a bioreactor.

In addition, we examined the viability properties against several eukaryotic cell lines, in order to see the effect of PFOA modification on other kinds of biomembranes, different from bacteria.

We also studied other properties of the modified chitosan film including degradation temperature, rheology and permeability to water vapor in view of its possible application as an overlay of bioreactors which could be subject to different conditions.

2. Experimental

2.1. Materials

Chitosan of low molecular weight (85% deacetylation degree) was obtained from Sigma–Aldrich (USA). Trifluoroacetic acid (TFA) 99.9%, pentafluoropropionic acid (PFPA) >97%, pentadecafluorooctanoic acid (PFOA) >90% (Fluka), acetic acid (HAc) 99.1% (Dorwill), 1,4-dioxane 99.9% and NaOH 97% (Cicarelli) were used as received. Purified deionized water from Millipore Milli-Q was used in all experiment.

2.2. Preparation of the films

Chitosan-PFOA films were prepared as follows: films of chitosan cast in acetic acid solution were previously prepared and extracted in NaOH 1 M for one day. It was then exhaustively washed with distilled water and dried at room temperature. Some of the films were kept as reference in the studies of pristine chitosan; the rest was immersed for a further day in solutions of PFOA in dioxane:H_2O (2:1) where the acid was totally dissolved. The swelling of chitosan, measured in a separate experiment in the same solvent mixture, was 90%. Films were afterwards washed with ethanol and dried at room temperature. The degree of substitution obtained under these conditions by gravimetric measurements was 80 mol% of PFOA.

For the TFA and PFPA acids another film preparation procedure was required because of dissolution of chitosan films in such acids. In this case, solutions of chitosan (1%, w/w) and its respective acid (TFA or PFPA) were prepared in 1:1 $-NH_2$:acid group ratio to minimize the effect of the degradation of the biopolymer chain resulting from an excess of acid. Different aliquots of the resultant solutions were poured into Petri dishes to get, by casting, films of diverse thickness according to the study performed (10 μm for IR analysis and 70 μm for the remaining studies).

In order to remove water absorbed, all the films were dried at 30 °C until constant weight. The water remaining in the samples comprises the adsorbed water subsequently released in the TGA tests. Samples for rheology were also dried at 60 °C one day before the measurements.

2.3. Spectroscopy characterization

Fourier transform infrared spectroscopy (FTIR) analysis of chitosan before and after modification was done in order to characterize the composition of the films. A Bruker IFS28 FTIR spectrophotometer was used to obtain spectra. FT-IR spectra were recorded in a spectral range of 4000–400 cm^{-1} with a resolution of 2 cm^{-1}; 4 scans were run for each sample. Those samples used for biological trial (ch-PFOA) were also evaluated by Fourier transform infrared attenuated total reflection spectroscopy (FTIR-ATR) in order to monitor the changes on the film surface. We used a Shimadzu FTIR-8501 spectrophotometer in a spectral range of 4000–400 cm^{-1} with a resolution of 2 cm^{-1}; 16 scans were performed for each sample.

2.4. Solid-state NMR measurements

Solid-state ^{13}C NMR cross-polarization (CP) and high-power decoupling (HPDEC) MAS NMR spectra were recorded on a Bruker Avance™ 400 spectrometer/imager (Bruker Analytik GmbH, Karlsruhe, Germany) equipped with a Bruker Ultra Shield™ 9.4-T (^1H resonance frequency of 400.14 MHz) (Instituto de Ciencia y Tecnología de Polímeros (ICTP), Spain). The 90° pulse lengths were 5.3 μs for ^{13}C. ^{13}C CP-MAS spectra were measured with 3 ms contact time, at room temperature, 5000 Hz spectral width and up to 4000 scans. During the detection period of the ^{13}C magnetization, dipolar decoupling was used to eliminate the large ^{13}C-^1H heteronuclear dipolar decoupling. The chemical shifts in ^{13}C spectra are referenced to TMS by using the methane carbon of solid adamantine (29.5 ppm) as an external reference standard.

2.5. Thermogravimetric effluent analysis by mass spectrometry (TGA-MS)

Thermogravimetric analysis was employed to compare the degradation characteristics of chitosan films chemically modified with untreated chitosan. The thermal stability of each sample was determined using a TGA Q500 thermogravimetric analyzer of TA Instrumental (Instituto de Ciencia y Tecnología de Polímeros (ICTP), Spain). It is hyphenated to a ThermoStar TM mass spectrometer, Pfeiffer vacuum with C-SEM, Channeltron detector in order to distinguish between the different gas species. TGA was performed in a range from 30 to 600 °C at a heating rate of 10 °C min^{-1} in a purified dynamic helium gas atmosphere. The MS range studied was 10–70 amu for all the samples and 70–130 amu (atomic mass units, m/z) for pristine chitosan only. A nitrogen purge of 50 mL min^{-1} was used in the furnace. The sample size of 11 mg was accurately weighed into an aluminum pan. Derivatograms of the TGA curves (DTG) were also recorded. In addition to the thermal stability provided by thermogravimetric analysis, information on the decomposition products of chitosan may be obtained if the effluent gases were analyzed by means of a supplementary technique such as mass spectrometry (MS).

2.6. Differential scanning calorimetry (DSC)

DSC thermograms were measured using a DSC from PerkinElmer model DSC7 connected to a temperature controller and interfaced to a thermal analysis data station (TADS). Once the films were dry, they were sealed in aluminum pans and heated at a rate of 10.0 K min^{-1}. During data collection, all experiments were done under a purge of dry nitrogen at a rate of 50 mL min^{-1}.

2.7. X-ray diffraction

X-ray diffraction patterns of chitosan before and after modification were collected in order to examine the crystalline state of the samples. They were taken in film form and analyzed by using a Bruker D8 Advance diffractometer system equipped with Global mirror and Vantec1 detector. The radiation was Cu Kα, λ = 1.54 Å, increase of 0.023851, scan speed 0.5 s, from 5° to 40° (2θ).

2.8. Morphology of chitosan films

AFM imaging was used to characterize the homogeneity of chitosan films obtained after chemical modification. AFM images of the samples were taken from Multimode Veeco Microscope, MMAFMLN model, 2078EX series, in tapping mode, at a resolution of 5 μm. The software used was Nanoscope 6.3. Height and phase images were recorded simultaneously. Surface corrugations are shown in height images. The fine structural details are displayed in the phase images which are sensitive to mechanical properties and chemical changes.

2.9. Contact angle

Contact angle determinations of the films were performed in order to assess the changes in the hydrofilicity of the samples before and after chitosan modification. The measurements were conducted with a home-made contact angle meter at ambient humidity and temperature. Droplets of deionized water were placed at different locations on the samples using a micro-syringe. The droplet volume was 4 μL. A minimum of eight readings was taken for each sample in order to determine average values. Typical standard deviations were 2–3°.

2.10. Rheology

The measurements of the dynamic mechanical properties E', E'' of plastic films in extension mode were performed using a Physica Rheometer Rheoplus/32, Anton Paar, Sanico, with a measuring system P-PTD200/l, 20.00 mm length (sample dimensions) between clamps and shaft and 10.00 mm width. The Software used was Rheoplus V 2.81.

2.11. Water vapor permeability

Water vapor permeability (WVP) of films was determined using aluminum dishes according to ASTM E 96-00 and E 104-02 methods for water vapor transmission of materials (desiccant method) and for maintaining constant relative humidity by means of aqueous solutions respectively. Films with an exposed area of 19 cm^2 were tested at 75% RH and 30 °C. Weight loss graphs were plotted with respect to time, and the linear least-square method was used to calculate water vapor transmission rate (WVTR) using the following equation:

$$\mathrm{WVTR} = \frac{\mathrm{slope}}{\mathrm{film\ area}}\ (\mathrm{g/h\ cm^2})$$

WVP was determined by using the following equation:

$$\mathrm{WVP} = \left(\frac{\mathrm{WVTR}}{\Delta P}\right) L = \left(\frac{\mathrm{WVTR}}{S}(R_1 - R_2)\right) L$$

where ΔP vapor pressure difference (Pa), S saturation vapor pressure at test temperature (Pa), R_1 relative humidity at the source expressed as a fraction, R_2 relative humidity at the vapor sink expressed as a fraction, and L as the average film thickness (cm).

2.12. Effect of chitosan and ch-PFOA films on cell monolayers

In order to evaluate the effect of the different films on cell viability we used the human epidermoid cancer cell line (Hep-2 – ATCC CCL 23). Cells were maintained in Eagle minimal essential media (MEM) supplemented with 10% fetal bovine serum (NATOCOR, Córdoba, Argentina), 2 mM L-glutamine (GIBCO) and with no antibiotics. Cells were grown routinely in 75 cm^2 flasks at 37 °C in a 5% CO_2 humidified atmosphere. Confluent stock cultures were trypsinized and new stock cultures were seeded with 10^5 cells/mL. For all experimental assays, 24-well tissue culture plate was used.

The cytotoxicity of chitosan and ch-PFOA films was evaluated on the basis of a procedure adapted from the ISO10993-5 standard test method. The films were prewashed with 70% ethanol for 30 min and washed 3 times with fresh culture medium prior to further incubation at 37 °C in fresh culture medium for 24 h. Then, a direct contact assay was used to evaluate cell adhesion and viability on the surface of ch-PFOA and chitosan membranes. For cell adhesion, membranes were placed in a 24-well plate and sterilized by ultraviolet (UV) irradiation for 30 min. Subsequently, 0.5 mL of cell suspension was seeded onto the sample surface; empty wells were also seeded with the same amount of cells to be used as controls and also to evaluate the effect of membranes on 24 h cell monolayers. All the seeded samples and controls were incubated for 24 h at 37 °C in an atmosphere containing 5% of CO_2. After this time, cell adhesion and proliferation were evaluated qualitatively by light microscopy. To observe cell proliferation on membranes, each sample was previously washed three times with sterile phosphate buffer solution (PBS) to remove non-adherent cells. Microscopic images of cell cultures exposed to the membranes were made by Axiovert 135 M. In addition, the effect of free PFOA on these cell lines was also examined. For this purpose, cell monolayers were incubated for 24 h with increasing concentrations of PFOA. Afterwards, the viability was assessed at each concentration.

Finally, we studied the interaction of PFOA, chitosan and ch-PFOA films with red blood cells (RBC). In these experiments, purified human red blood cells at 5% in saline solution were incubated for 2 h at room temperature with chitosan and ch-PFOA films and with increasing concentration of free PFOA. Aliquots of samples were taken at various time periods and the percentage of hemolysis measuring free hemoglobin was quantified by UV–vis spectrophotometry at 540 nm.

2.13. Bacterial viability assessment on chitosan and ch-PFOA films

P. aeruginosa ATCC 27853 strains (from the American Type Culture Collection) were cultured overnight on ch-PFOA and chitosan films in Brain heart broth (Merck 1.10493) at 37 °C. The culture was centrifuged at 3000 rpm × 5 min and washed with sterile PBS. Cells were re-suspended to an optical density at 600 nm of 1, and then diluted in PBS corresponding to 10^3 or 10^7 colony-forming unit/mL respectively.

Chitosan and ch-PFOA films (0.5 cm diameter) were prepared in triplicate and soaked in 1 mL of bacterial suspension in 48-well culture dish for 5 h or 24 h at 50 rpm, 25 °C.

After the treatments, 100 μL of each sample and decimal dilutions were cultured in Petri dish containing Brain heart broth (Merck 1.10493) with 1.5% of Select agar (Gibco 30391-023) and supplemented with 0.01% (w/v) of 2,3,5-triphenyltetrazolium chloride (TTC) widely used in biology as indicators of metabolic activity, hence termed vital dyes [15].

Following the pour-plate technique described in the standard methods for the examination of water and wastewater (21° Edition), the period of incubation ranged from 24 to 48 h at 37 °C, with each colony being directly counted to determine the total number

of colony-forming units (CFUs) on the plates. Finally, by multiplying this count by the total dilution factor it was possible to find the total number of CFUs in the original samples.

3. Results and discussion

3.1. Spectroscopy film characterization

Films prepared by casting of different acid solutions, ch-HAc, ch-TFA, ch-PFPA, ch-PFOA, were spectroscopically characterized by IR and RMN. The main absorption bands of chitosan can be seen at 1653 and 1585 cm^{-1} corresponding to the primary amino groups (see the spectra in the supporting information). After modification with fluoride acids, amino bands decreased and were overlaid by two new bands in this region around 1678 and 1532 cm^{-1} corresponding to the presence of the perfluoroalkyl acid in the chitosan film as amine salts. Furthermore, bands between 1330 and 1028 cm^{-1}, and in the region between 840 and 530 cm^{-1}, showed fluorinated carbonic acid. These absorption bands disappeared by alkali treatment of the film, as reported by other authors [9].

^{13}C {1H} CP MAS RMN spectra of pure chitosan film recorded after casting of the different acids analyzed support the findings of the IR studies (see the spectra in the supporting information). In the presence of the fluorinated acids, a new peak appeared at 163 ppm corresponding to the formation of amine salts, having a fluoroalkyl group in its immediate neighborhood. Furthermore, the corresponding fluorinated carbons appeared between 90 and 120 ppm.

3.2. Thermal characterization

The thermal stability of the films was studied by TGA-MS. Fig. 1a and b shows the TG and its differential curves for chitosan and its derivatives recorded in nitrogen. Two main ranges were observed, the first (30–200 °C) corresponds to solvent evaporation: this process is found to be lower in temperature and in weight loss when fluoride substitute is present, which further decreases when fluoride chain is longer in the TFA > PFPA > PFOA sequence. This result suggests lower water retention due to substitution of amino groups with increased long-chain fluorinated pending, most evident in ch-PFOA. The second main range found (200–400 °C) corresponds to the thermal degradation of polymer chains. Only one peak is observed in the derivative curve of chitosan (Fig. 1b), while it splits in more degradation processes in the substituted samples when the fluoride carbon chain increases. It is also observed that, in the case of fluoride derivatives (between 290 and 233 °C), degradation temperature and residue percentage decrease compared with pristine chitosan (303 °C). Temperatures and weight loss (%) are summarized in the supporting information. These findings show the destabilization of polymer chains due to the loss of the initial hydrogen-bridge interaction.

The apparent activation energy for the thermal degradation of chitosan and its derivatives was determined from the TG curves using the method described by Broido [16,17].

This equation can be written in the form of:

$$\ln\left[\ln\left[\frac{1}{(1-\alpha)}\right]\right] = -\frac{E_a}{RT} + \ln\left[\left(\frac{R}{E_a}\right)\left(\frac{Z}{U}\right)\right] \quad (1)$$

α is the extent of conversion and is given by:

$$\alpha = \frac{W_e}{W_o}$$

where W_e is the mass of polymer evolved as volatile fragments and W_o is the initial mass, R the gas constant, Z the constant, T_m the temperature of the maximum reaction velocity and U the rate of heating.

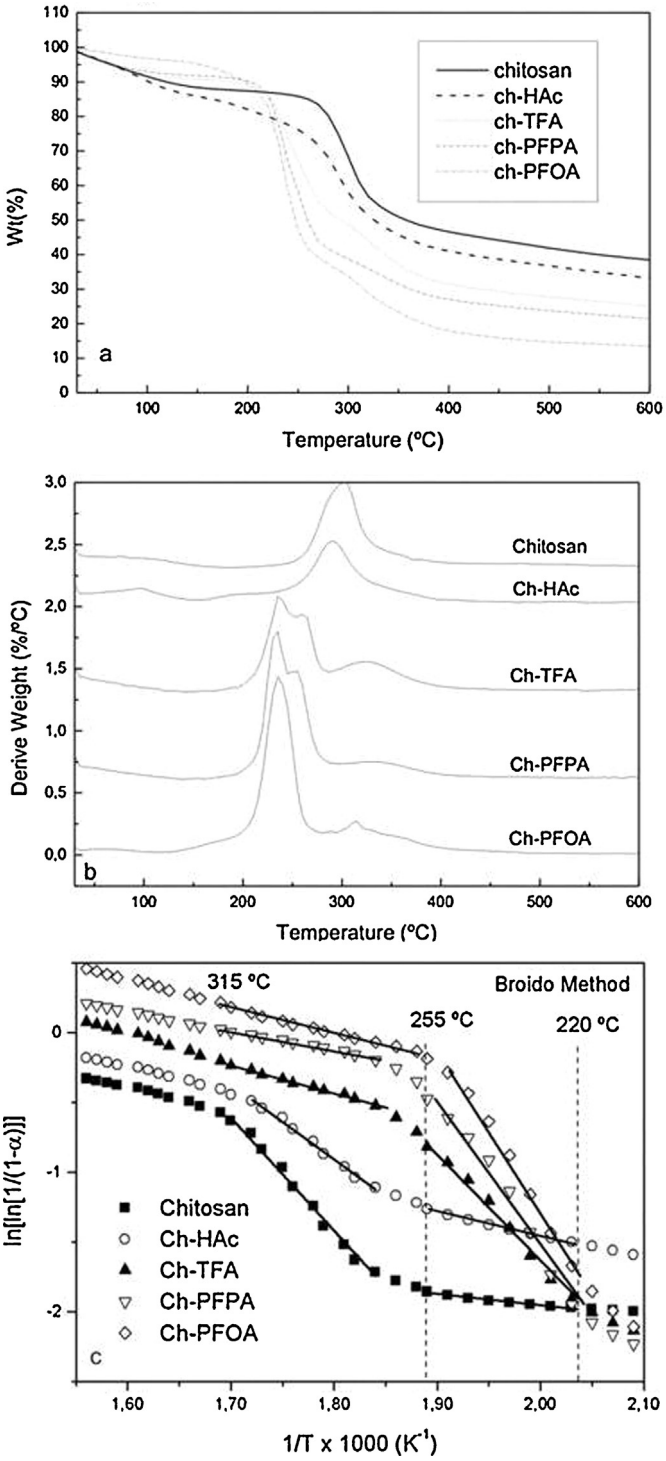

Fig. 1. (a) TG curves of chitosan and its derivatives; (b) derive weights curves of chitosan and its derivatives; (c) plots of $\ln\left[\ln[1/(1-\alpha)]\right]$ vs. $10^3\,T^{-1}\,(K^{-1})$ using Broido method for chitosan and its derivatives during thermal degradation.

Fig. 1c shows plots of $\ln\left[\ln[1/(1-\alpha)]\right]$ vs. $1/T$ for the temperature range 220–315 °C, corresponding to the second degradation step. Linear plots are obtained with different slopes indicating three temperature regions of degradation. The values of the apparent activation energies (E_a) were determined from the slopes of these plots. Table 1 reports the E_a and weight loss data gathered for the two degradation periods. Chitosan was almost not degraded in Period I (220–260 °C), since only 1.5% weight was lost with an

Table 1
Activation energies and weight loss in dynamic TG analysis during the termal degradation of chitosan and its derivatives (Broido method) (mean ± SD, $n = 3$).

Sample	Period I (220–260 °C)		Period II (260–315 °C)	
	E_a (kJ mol^{-1})	Weight loss (%)	E_a (kJ mol^{-1})	Weight loss (%)
Chitosan	5.9	1.5	74.1	26.9
ch-HAc	14.9	4.6	42.8	22.9
ch-TFA	64.3	21.6	18.1	19.2
ch-PFPA	87.4	32.7	11.5	17.3
ch-PFOA	98.2	38.9	16.2	13.6
Interpretation	Degradation of side chains		Degradation of chitosan chains	

Table 2
Mass fragments produced during the thermal degradation of chitosan and its derivatives.

m/z (temperature, °C)					
Chitosan	Ch-HAc	Ch-TFA	Ch-PFPA	Ch-PFOA	Assignment
		12 (260)	12 (255)	12 (245)	C^+ [a]
			31 (260)	31 (255)	CF^+
	41(390)				$COCH^+$, CH_3CN^+ [a]
		44 (260)	44 (255)	44 (250)	CO_2^+
				45 (245)	$C_2H_5O^+$, $C_2H_7N^+$
				47 (250)	$C_2H_5OH_2^+$, $CH(OH)_2^+$
		50 (260)	50 (260)	50 (255)	CF_2^+
		51 (260)	51 (260)	51 (250)	CHF_2^+
		52 (260)	52 (255)	52 (255)	$CH_2F_2^+$
53(340)					$C_4H_5^+$
			62 (265)	62 (245)	$C_2H_6O_2^+$
			63 (260)	63 (255)	$C_5H_3^+$, $C_2H_7O_2^+$
				66 (250)	$C_5H_6^+$
				67 (250)	$C_5H_7^+$, $C_4H_3O^+$
		68 (260)		68(250)	$C_5H_8^+$, $C_4H_4O^+$, $C_3H_6CN^+$
		69 (260)	69 (260)	69 (255)	CF_3^+
		70 (260)	70 (260)	70 (250)	$C_5H_{10}^+$, $C_4H_6O^+$, $C_3H_8N^+$, CF_3H^+
80(320)					$C_6H_8^+$, $C_5H_4O^+$, $C_5H_6N^+$

[a] Quijada-Garrido et al. [18].

E_a value of 5.9 kJ mol^{-1}. E_a and weight loss of chitosan derivatives increased with the length of fluorinated chain from 64.3 to 98.2 kJ mol^{-1}, resulting from the breakdown of the fluorinated pendant chains to raise fluorinated mass fragments (Table 2). In this period, the stability of the fluorinated chain substituent increases with a longer chain, therefore increasing E_a. However, in Period II (260–315 °C), the opposite tendency is observed. During this step of the process, a value of 74.1 kJ mol^{-1} for E_a was obtained in the case of chitosan alone which decreased to 16.2 kJ mol^{-1} for ch-PFOA. In this case degradation occurs in the main polymer chain, which is further destabilized with release of the longest acid fluoride chain; energy cost is thus lower. Fig. 1c indicates a third temperature region (>315 °C) over Period II, with all samples having lower E_a values (lower slopes) than those found in Period II.

Table 2 shows all the mass fragments observed as well as the assignment in the mass interval detected up to 70 amu. In the case of chitosan and ch-HAc, only few fragments are seen, fragment 41 being the most important. This segment corresponds to acetamide from the chitosonium acetate unit NH_3^+-OOC-CH_3 by a simultaneous elimination reaction with ammonia or water, giving place to CHCO or CH_3CN fragments respectively [18] at a maximum of 390 °C. However, for ch-TFA, ch-PFPA and ch-PFOA, the fragments observed: m/z, 31 CF^+; 44 CO_2^+; 50 CF_2^+; 51 CHF_2^+; 52 $CH_2F_2^+$; 69 CF_3^+; 70 CF_3H^+, correspond to the fluoride acid used as modifier, which arise in the temperature range of 250–260 °C corresponding to the first period of degradation. In these samples we can find other fragments arising from the earlier decomposition of glucosaminic ring due to lowest degradation temperature. In the supporting information we can see the overlapping of the relative intensities of main mass fragments as well as the relative intensities and TG curve for chitosan and its derivatives.

DSC shows an exothermic transition which T_{max} coincided with the degradation temperature. The same tendency is observed in TG studies (see Table 3 in the supporting information). In addition, no glass transition is found, neither in pure nor modified chitosan.

3.3. X-ray diffraction

Fig. 2 displays the X-ray diffraction patterns of the films. The diffractograms of chitosan film exhibit two major crystalline peaks (2θ) around 10° and 20° in agreement with previously reported

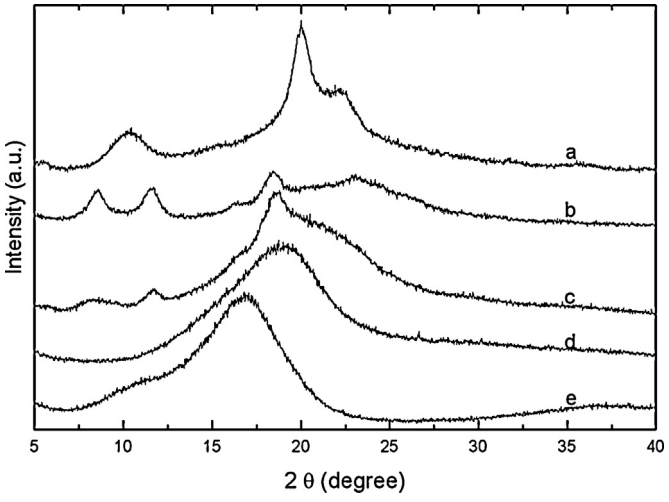

Fig. 2. X-ray diffraction patterns of modified chitosan films. (a) Chitosan; (b) ch-HAc; (c) ch-TFA; (d) ch-PFPA; (e) ch-PFOA.

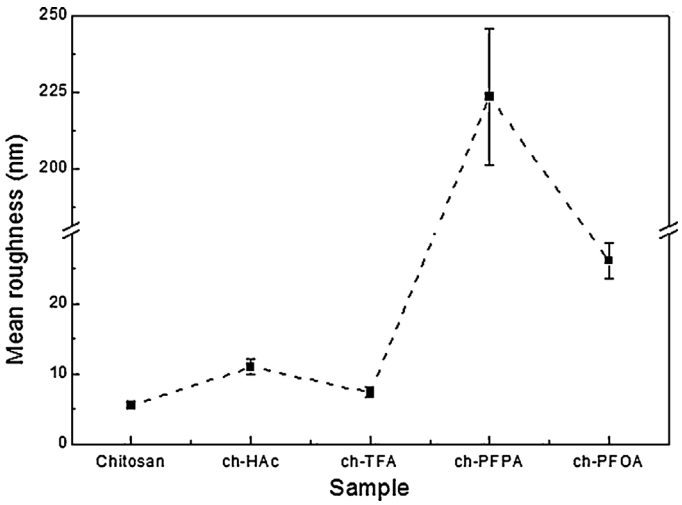

Fig. 3. Comparative mean roughness in chitosan and its derivatives (mean ± SD, $n = 5$).

results [8,19,20]. The characteristic peaks of chitosan disappear in the presence of the acids. For HAc and TFA new peaks appear around 8°, 12° and 18°. However, significant changes in crystallinity are found for PFPA and PFOA where an amorphous hump is seen around 17° and 19° respectively. The rigid crystalline structure of pure chitosan is stabilized mainly by intra and intermolecular hydrogen bonds. When glucosamine units in chitosan membranes are modified, hydrogen bonding involving the NH_2 groups is disrupted, so the rigid crystalline structure weakens. In the ch-PFOA sample, a new signal appears at 10°, which could be related to a partial rearrangement of the hydrophobic chains.

3.4. AFM analysis

Fig. 3 shows the surface roughness obtained from height and phase images of chitosan and acid-modified chitosan film. Chitosan film presents morphologic features for crystalline polymers. The introduction of HAc, TFA or PFPA to chitosan modified the structure which became smoother in the case of TFA (see the images in the supporting information). The maximum roughness was observed for ch-PFPA followed by ch-PFOA; however, both are higher than chitosan film alone.

These results agree with those of X-ray studies, where diffractograms show the disappearance of the chitosan crystal structure in the modified samples, especially when PFPA is added. This could indicate that such material may be the beginning of phase segregation or rearrangement of the hydrophobic chains to the surface. By increasing chain length (ch-PFOA), the hydrophobic chains are rearranged in hydrophobic domains clearly defined by X-rays, resulting in a decrease in surface roughness.

3.5. Contact angle

The contact angle of drops of water on chitosan, ch-TFA, ch-PFPA and ch-PFOA films was analyzed. From all films studied, the only reliable result of contact angle obtained was for ch-PFOA, on which the drop remained stable ($\theta = 92°$). By contrast, chitosan film presented swelling and ch-TFA/ch-PFPA films presented dissolution, all of them revealing surface hydrophilic characteristics. Therefore, the ch-PFOA sample showed the highest surface stability compared to the other samples studied. The slightly hydrophobic character of ch-PFOA, considering its contact angle, is ascribed to the fact that chitosan keeps its hydroxyl groups unmodified after PFOA addition, providing it with most of its hydrophilicity. In spite of that, and as

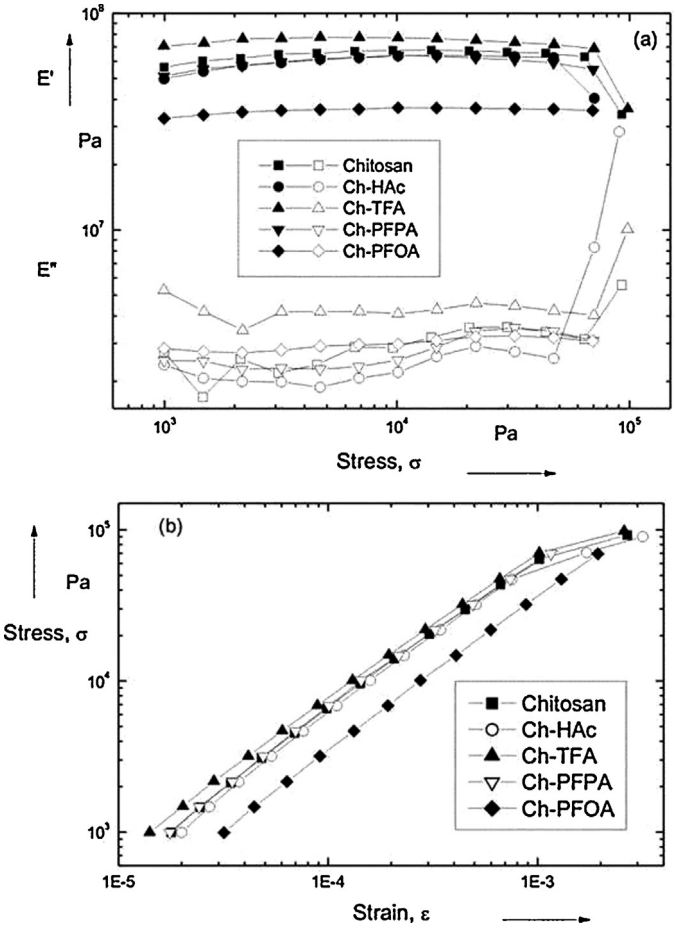

Fig. 4. Rheological studies of films of chitosan and derivatives: (a) plot store (E') and loss modules (E'') vs. stress (σ); (b) plot stress (σ) vs. strain (ε).

described below, we see that PFOA produces noticeable changes in the properties of chitosan, such as surface stability in aqueous media, facilitating bacterial adhesion. For qualitative comparison, the images of water drops on chitosan, ch-PFPA and ch-PFOA films are provided in the supporting information.

3.6. Rheology

Fig. 4 exhibits the rheological measurements performed on chitosan films and its derivatives. In plot (a), store (E') and loss modulus (E'') vs. Stress (σ) is represented, and in plot (b), stress (σ) vs. strain (ε) is shown. From these results, it is observed that chitosan preserves its rheological properties, even after modification in most samples. In the case of ch-PFOA, a decrease in the modulus is observed; this material then turns into a more flexible film compared to that of the other samples.

3.7. Study of the properties of ch-PFOA films

3.7.1. Water-vapor barrier

The water-vapor permeability (WVP) was determined for the sample chitosan, ch-HAc and ch-PFOA, by the desiccant method and the equations described in the experimental part. The results obtained were 1.13×10^{-12}, 1.01×10^{-12} and 0.85×10^{-12}, respectively, given in g/Pa s m. units. A noticeable decrease in the WVP of ch-PFOA (25%) was seen in relation to chitosan. This result reveals a decrease in the water permeability of chitosan modified through PFOA substitution. The samples obtained with the other fluoride

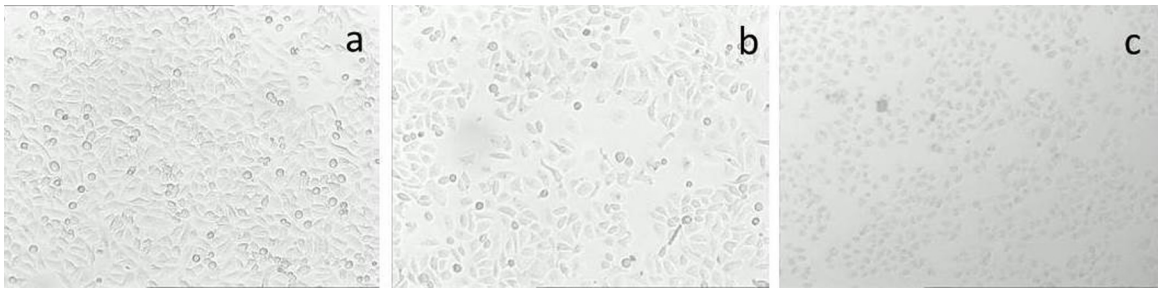

Fig. 5. Microscopic images of Hep2 cell culture: (a) medium used as control; (b) medium after direct contact with chitosan membrane; (c) medium after direct contact with chit-PFOA membrane.

acids could not be measured due to dissolution of the membrane in wet atmospheric conditions.

3.7.2. Effect on cell monolayers

The in vitro biocompatibility of chitosan and ch-PFOA films was evaluated to ascertain their impact, if any, on supporting the growth and proliferation of the cells. With chitosan films, no toxic effect was observed on Hep-2 cells; cell viability remained unaltered following control after 24 h in culture. In contrast, ch-PFOA showed high toxicity on these cells (Fig. 5). Similar results were obtained with cells incubated with free PFOA, suggesting that the results described above for ch-PFOA would be related to the PFOA molecules associated with the film. The same results were found with VERO (African green monkey kidney cells) and Caco (human epithelial colorectal adenocarcinoma) cells (data not shown). In order to clarify this point we performed the FTIR-ATR spectra of the membranes before and after their exposure to the cells. The pattern of the superficial level of the films showed a decrease from 0.65 to 0.40 of the PFOA absorption bands of 1393 cm^{-1} in relation to the 1031 cm^{-1} band of chitosan (reference band) after cell exposure to the films. This observation shows a direct action of the substituent on cell membranes, either released or generated by the disruption of the bilayer from the film itself.

In other experiments, about 10% of lysis was observed next to the incubation of ch-PFOA films with red blood cells (RBC). This effect is probably due to PFOA, since chitosan membranes have no lytic effect whereas free PFOA causes 30% lysis of RBC.

3.7.3. Bacterial viability assessment

Fig. 6 shows the results obtained from the incubation of bacteria *P. aeruginosa* with different initial amounts of colony-forming units (10^7 or 10^3 CFUs) in the presence of ch-PFOA films. It is observed that the concentration of bacteria in suspension decreases substantially in both inocula in relation to the chitosan film alone. The decrease in the number of colonies in suspension is attributed to the adhesion of bacteria to the film of ch-PFOA, evidenced by the dark-coloring that the films acquire in the presence of the metabolic indicator added (data not shown). The formation of a biofilm can also be observed. These facts are not observed in the chitosan film alone. Contrarily to what happens with monolayer cells, bacterial viability is not affected by PFOA. Previous reports have attempted to elucidate the relationship between the bioadhesive properties of membranes with roughness, membrane potential or hysteresis in the contact angle [12,14]. Terada et al. [12] found that electrostatic interactions and an increased surface area facilitate the initial bacterial adhesion. In addition, a more recent publication [21] reports on the different models, known up to now, that try to explain the mechanism and control of bacterial adhesion. Several kinds of interactions such as van der Waals, acid–base, hydrophobic ones can be operating, in addition to others inherent to cell surface structures. This turns actual bacterial adhesion into a highly complex process.

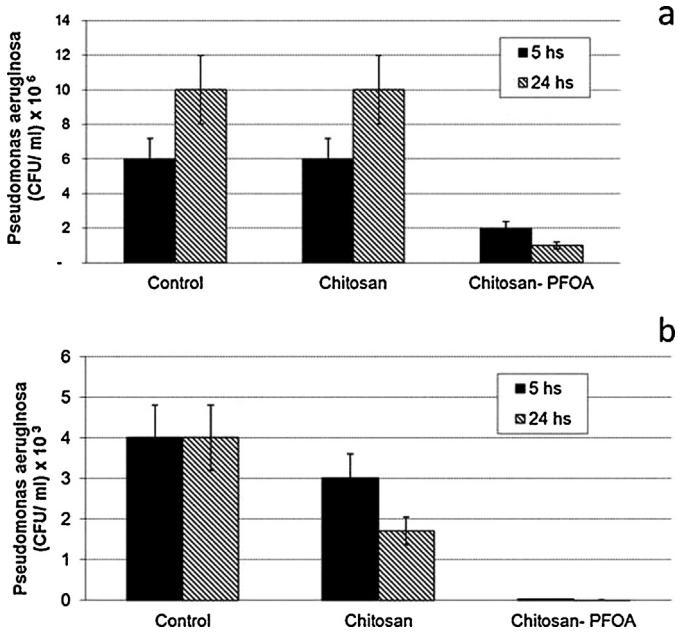

Fig. 6. Total number of colony forming units (CFU/mL) of bacteria *Pseudomonas aeruginosa* onto the chitosan and ch-PFOA for 5 h and 24 h for an initial (a) 10^7 and (b) 10^3 CFUs, respectively (mean ± SD, $n = 3$). Control refers to the bacteria culture without the presence of any membrane.

In our work, what we observe is that ch-PFOA films promote adhesion of the colonies with a concomitant decrease in the bacterial count in suspension and consequent formation of a biofilm. The process by which this phenomenon takes place could involve a combination of surface characteristics, such as roughness and wettability, which helps providing a very stable and rheological improved material with bacterial adhesion properties.

4. Conclusions

Chitosan films with different characteristics were obtained depending on the type of the fluorocarbon acid added as modifier. In the case of chitosan with TFA, the film displayed the highest hydrophilicity due to the formation of highly soluble salt. In the case of PFPA, the hydrophilicity has also been shown to be significant but in a decreasing rate, giving as a result a particularly amorphous material with enhanced rugosity. By contrast, when PFOA is added, hydrophobic interactions prevail, causing an increase in the contact angle, and a decrease in water permeability.

In the thermal studies, the degradation temperature decreases progressively with the incorporation of more hydrophobic acid, producing a destabilization of the structure by the addition of fluorinated side groups that interfere in the hydrogen bonds between original chitosan chains. Apparently, the chain of ch-PFPA sets a

limit for the changes from hydrophilic to hydrophobic interactions between chains of modified chitosan, since PFPA contributes to breaking hydrogen-bridge interactions between chains, yielding a soluble material in water. However, in the case of PFOA as modifier, hydrophobic interactions prevail over hydrophilic ones, the product losing its solubility in water. In this case, an amorphous character and the appearance of a new signal, probably related to a partial rearrangement of the hydrophobic chains, are observed by X-ray diffraction. However, the changes in the morphology and hydrophobic/hydrophilic interactions practically do not affect the rheological properties of the films, except ch-PFOA, turned into more flexible films compared to the other samples.

Furthermore, it was demonstrated that the modified ch-PFOA films significantly affect the lipid bilayers, as evidenced by the lysis observed with red blood cells and the toxicity demonstrated in various cell lines (Caco, Hep2 and Vero). However, the interaction established with the polysaccharide wall of bacteria is completely different, where a marked adhesive effect is seen. In this particular case, ch-PFOA film has no electric charge, whereupon the electrostatic interaction does not take place between prokaryotes and the film. Therefore we conclude that the phenomenon of bacterial adhesion can be ascribed, on the one hand, to other interactions such as van der Waals, hydrophobic ones, etc., and on the other, to the roughness that could be promoting it.

Acknowledgements

The authors acknowledge the financial support provided by Agencia Nacional de Promoción Científica y Tecnológica (ANPCyT) and Consejo Nacional de Investigaciones Científicas y Técnicas (CONICET). Dr. Karina Bierbrauer also thanks the technicians from the Instituto de Ciencia y Tecnología de Polímeros (ICTP), Spain, for technical support.

Appendix A. Supplementary data

Supplementary data associated with this article can be found, in the online version, at http://dx.doi.org/10.1016/j.colsurfb.2013.10.013.

References

[1] C. Mao, W.B. Zhao, A.P. Zhu, J. Shen, S.C. Lin, Process Biochem. 39 (2004) 1151.
[2] A. Gandini, Macromolecules 41 (2008) 9491.
[3] K. Fink, S. Höhne, S. Spange, F. Simon, J. Adhes. Sci. Technol. 23 (2009) 297.
[4] K.S. Chow, E. Khor, Carbohydr. Polym. 47 (2002) 357.
[5] J.J. Resinger, M.A. Hillmyer, Prog. Polym. Sci. 27 (2002) 971.
[6] S. Höhne, R. Frenzel, A. Heppe, F. Simon, Biomacromolecules 8 (2007) 2051.
[7] A.G. Cunha, A. Gandini, Cellulose 17 (2010) 1045.
[8] M. Hasegawa, A. Isogai, F. Onabe, M. Usuda, J. Appl. Polym. Sci. 45 (1992) 1857.
[9] M. Hasegawa, A. Isogai, F. Onabe, M. Usuda, R.H. Atalla, J. Appl. Polym. Sci. 45 (1992) 1873.
[10] T. Karlen, D. Chambettaz, US Patent No. 6,264,929, (2001).
[11] J. He, R.L. Baldini, E. Dëiziel, M. Saucier, Q. Zhang, N.T. Liberati, D. Lee, J. Urbach, H.M. Goodman, L.G. Rahme, PNAS 101 (2004) 2530.
[12] A. Terada, A. Yuasa, S. Tsuneda, A. Hirata, A. Katakai, M. Tamada, Colloids Surf. B 43 (2005) 99.
[13] C. Díaz, P.L. Schilardi, P.C. dos Santos Claro, R.C. Salvarezza, M.A. Fernández Lorenzo de Mele, ACS Appl. Mater. Interfaces 1 (2009) 136.
[14] E.H. Sohn, J. Kim, B.G. Kim, J.I. Kang, J.S. Chung, J. Ahn, J. Yoon, J.C. Lee, Colloids Surf. B 77 (2010) 191.
[15] L. Ping, D.A.I. Mavridou, E. Emberly, M. Westermann, S.J. Ferguson, PLoS ONE 7 (2012) e38427.
[16] A.J. Broido, Polym. Sci. A-2 7 (1969) 1761.
[17] X. Qu, A. Wirsén, A.C. Albertsson, Polymer 41 (2000) 4841.
[18] I. Quijada-Garrido, V. Iglesias-González, J.M. Mazón-Arechederra, J.M. Barrales-Rienda, Carbohydr. Polym. 68 (2007) 173.
[19] P. Sangsanoh, P. Supaphol, Biomacromolecules 7 (2006) 2710.
[20] M.M. Beppu, R.S. Vieira, C.G. Aimoli, C.C. Santana, J. Membr. Sci. 301 (2007) 126.
[21] K. Hori, S. Matsumoto, Biochem. Eng. J. 48 (2010) 424.